



**HAL**  
open science

## Acetaminophen metabolism revisited using non-targeted analyses: Implications for human biomonitoring

Arthur David, Jade Chaker, Thibaut Léger, Raghad Al-Salhi, Marlene Dalgaard, Bjarne Styrishave, Daniel Bury, Holger Koch, Bernard Jégou, David Kristensen

### ► To cite this version:

Arthur David, Jade Chaker, Thibaut Léger, Raghad Al-Salhi, Marlene Dalgaard, et al.. Acetaminophen metabolism revisited using non-targeted analyses: Implications for human biomonitoring. *Environment International*, 2021, 149, pp.106388. 10.1016/j.envint.2021.106388 . hal-03630174

**HAL Id: hal-03630174**

**<https://hal.ehesp.fr/hal-03630174>**

Submitted on 4 Apr 2022

**HAL** is a multi-disciplinary open access archive for the deposit and dissemination of scientific research documents, whether they are published or not. The documents may come from teaching and research institutions in France or abroad, or from public or private research centers.

L'archive ouverte pluridisciplinaire **HAL**, est destinée au dépôt et à la diffusion de documents scientifiques de niveau recherche, publiés ou non, émanant des établissements d'enseignement et de recherche français ou étrangers, des laboratoires publics ou privés.

# Acetaminophen metabolism revisited using non-targeted analyses: implications for human biomonitoring

Arthur David<sup>1\*</sup>, Jade Chaker<sup>1</sup>, Thibaut Léger<sup>1</sup>, Raghad Al-Salhi<sup>1</sup>, Marlen D. Dalgaard<sup>2</sup>, Bjarne Styrihave<sup>3</sup>, Daniel Bury<sup>4</sup>, Holger M. Koch<sup>4</sup>, Bernard Jégou<sup>1,‡</sup>, David M. Kristensen<sup>1,5,‡</sup>

## Affiliations:

<sup>1</sup>Univ Rennes, Inserm, EHESP, Irset (Institut de recherche en santé, environnement et travail) - UMR\_S 1085, F-35000 Rennes, France.

<sup>2</sup>Department of Health Technology, Technical University of Denmark, Denmark.

<sup>3</sup>Department of Pharmacy, Faculty of Health and Medical Sciences, University of Copenhagen, Denmark.

<sup>4</sup>Institute for Prevention and Occupational Medicine of the German Social Accident Insurance – Institute of the Ruhr-University Bochum (IPA), Bürkle-de-la-Camp-Platz 1, 44789 Bochum, Germany.

<sup>5</sup>Danish Headache Center, Department of Neurology, Rigshospitalet-Glostrup, Denmark.

\*Corresponding author: Arthur David ([arthur.david@ehesp.fr](mailto:arthur.david@ehesp.fr))

‡Joint last authors

**Abstract:**

The analgesic paracetamol (N-acetyl-4-aminophenol, APAP) is commonly used to relieve pain, fever and malaise. While sales have increased worldwide, a growing body of experimental and epidemiological evidence has suggested APAP as a possible risk factor for various health disorders in humans. To perform internal exposure-based risk assessment, the use of accurate and optimized biomonitoring methods is critical. However, retrospectively assessing pharmaceutical use of APAP in humans is challenging because of its short half-life. The objective of this study was to address the key issue of potential underestimation of APAP use using current standard analytical methods based on urinary analyses of free APAP and its phase II conjugates. The question we address is whether investigating additional metabolites than direct phase II conjugates could improve the monitoring of APAP. Using non-targeted analyses based on high-resolution mass spectrometry, we identified, in a controlled longitudinal exposure study with male volunteers, overlooked APAP metabolites with delayed formation and excretion rates. We postulate that these metabolites are formed via the thiomethyl shunt after the enterohepatic circulation as already observed in rodents. Importantly, these conjugated thiomethyl metabolites were (i) of comparable diagnostic sensitivity as the free APAP and its phase II conjugates detected by current methods; (ii) had delayed peak levels in blood and urine compared to other APAP metabolites and therefore potentially extend the window of exposure assessment; and (iii) provide relevant information regarding metabolic pathways of interest from a toxicological point of view. Including these metabolites in future APAP biomonitoring methods therefore provides an option to decrease potential underestimation of APAP use. Moreover, our data challenge the notion that the standard methods in biomonitoring based exclusively on the parent compound and its phase II metabolites are adequate for human biomonitoring of a non-persistent chemical such as APAP.

**Key words**

Paracetamol/acetaminophen; human biomonitoring, non-targeted analyses, high-resolution mass spectrometry (HRMS).

## Chemical abbreviations

APAP=acetaminophen; APAP-S=APAP sulfate; APAP-Glu=APAP glucuronide; NAPQI=N-acetyl-*p*-benzoquinone imine; 3-OH-APAP=3-hydroxyacetaminophen; 3-OH-APAP-S=3-hydroxyacetaminophen sulfate; 3-OCH<sub>3</sub>-APAP=3-methoxyacetaminophen; 3-OCH<sub>3</sub>-APAP-Glu=3-methoxyacetaminophen glucuronide; APAP-SG=acetaminophen glutathione; APAP-Cys= 3-(Cystein-S-yl)acetaminophen ; NAC-APAP= Acetaminophen mercapturate; NAC-O-APAP= Acetaminophen mercapturate sulfoxide; SH-APAP= 3-mercaptoacetaminophen; SH-APAP-Glu= 3-mercaptoacetaminophen glucuronide; SH-APAP-S= 3-mercaptoacetaminophen sulfate; S-CH<sub>3</sub>-APAP= S-methyl-3-thioacetaminophen; S-CH<sub>3</sub>-APAP-S= S-methyl-3-thioacetaminophen sulfate; S-CH<sub>3</sub>-APAP-Glu= S-methyl-3-thioacetaminophen glucuronide; SO-CH<sub>3</sub>-APAP= S-methyl-3-thioacetaminophen sulphoxide ; SO-CH<sub>3</sub>-APAP-S= S-methyl-3-thioacetaminophen sulphoxide sulfate; SO-CH<sub>3</sub>-APAP-Glu= S-methyl-3-thioacetaminophen glucuronide.

## 1 INTRODUCTION

2 The mild analgesic paracetamol/acetaminophen (N-acetyl-4-aminophenol, APAP) is an active  
3 ingredient in more than 600 prescription and non-prescription pharmaceuticals (Hurwitz et al., 2014).  
4 This analgesic is one of the most commonly used pharmaceuticals worldwide, with sales that have  
5 steadily increased over the past 20 years in several countries (Kristensen et al., 2016). The medical  
6 benefits of APAP are widely recognized; APAP can be used on its own, in mixed formulations or as an  
7 alternative to non-steroidal anti-inflammatory drugs whose suspected negative side effects have  
8 raised concerns (Kristensen et al., 2018). However, recent experimental as well as epidemiological  
9 studies suggest APAP as a possible risk factor for male developmental disorders in humans, on its  
10 own, or in combination with other reproductive and developmental toxicants (Albert et al., 2013;  
11 Konkel, 2018; Kortenkamp, 2020; Kortenkamp and Koch, 2020; Kristensen et al., 2012; Kristensen et  
12 al., 2016). Furthermore, incorrect use of APAP is strongly associated with a broad spectrum of side  
13 effects and is the most common cause of acute liver failure (fulminant liver failure) with over 100,000  
14 cases alone in the US (Ferri, 2016).

15 Besides APAP exposure through intentional pharmaceutical use, it has been shown that APAP is  
16 ubiquitously excreted in the urine of non-users in the general population (medians of 61.7 µg/L and  
17 100 µg/L from the German (men and women) (Modick et al., 2014) and Danish (women and children)  
18 (Nielsen et al., 2015) populations, respectively), indicating that an unintentional environmental  
19 exposure exists. The environmental exposure has been linked to APAP precursors such as aniline and  
20 4-aminophenol (two large-volume intermediates in industrial processes) and/or indirect APAP  
21 exposure through environmental sources (Kristensen et al., 2016; Modick et al., 2014; Modick et al.,  
22 2016). The APAP urinary background concentrations measured in non-users are about 4000 fold  
23 lower than the maximum urinary concentrations measured after oral intake of 500 mg APAP, but in  
24 the range of concentrations measured 24-48h after such an intentional oral intake (Modick et al.,

1 2014). Hence, these environmental APAP urinary concentrations can interfere when assessing APAP  
2 use in epidemiological studies especially if intentional APAP intake occurred >24h before sampling.

3 Understanding the amount of a chemical that enters the human body, whether from intentional use  
4 or unintentional exposure, is essential for both exposure and risk assessment. APAP metabolism is  
5 rapid (half-life <3h in blood (Mazaleuskaya et al., 2015)) and the large majority of the APAP  
6 therapeutic dose is classically believed to be excreted in urine as direct phase II glucuronide and  
7 sulfate conjugates. Mercapturic acid and cysteine conjugates derived from glutathione conjugation  
8 of the reactive metabolite N-acetyl-p-benzoquinone imine (NAPQI) are also produced in APAP  
9 metabolism. However, these metabolites are generally considered as minor metabolites together  
10 with catechol metabolites produced by CYP450 enzymes (Bessems and Vermeulen, 2001;  
11 Mazaleuskaya et al., 2015). Thus, present standard targeted methods analyzing free APAP and the  
12 phase II conjugates as “total APAP” after enzymatic deconjugation have been considered as the valid  
13 standard methods for estimating internal exposure for risk assessment purposes (Bornehag et al.,  
14 2018; Modick et al., 2014; Nielsen et al., 2015). However, these methods capture only part of the  
15 metabolic pathway and a relatively short time window to assess APAP origin (i.e. pharmaceutical use  
16 versus environmental), leading to potential underestimations of actual exposures. Exposure  
17 underestimations may have large implications as they could fundamentally compromise outcomes of  
18 risk assessment decisions.

19 In this study, we address the key issue of potential underestimation of APAP use using current  
20 human-biomonitoring methods focused on free APAP and phase II conjugates, only. We monitored  
21 APAP exposure over four days in blood and urine of four male volunteers with an administration of 1  
22 gram of APAP on the third day. Using recent untargeted technological advancements of high-  
23 resolution mass spectrometry (HRMS) combined with omics-based data treatment, we investigated  
24 the presence of up to now largely neglected APAP metabolites from enterohepatic circulation with  
25 formation and excretion times potentially longer than APAP. Such additional knowledge can improve

1 the human biomonitoring approach for the non-persistent chemical APAP in future exposure and risk  
2 assessment studies.

3

#### 4 **MATERIALS AND METHODS**

##### 5 *Longitudinal clinical trial*

###### 6 *Design and participants*

7 The human in vivo study (n=4) was designed as a longitudinal exposure to APAP over four days with  
8 an administration of 1 gram of APAP on the third day (Fig S1.). The study protocol was in compliance  
9 with the Helsinki Declaration and was approved by the Regional Scientific Ethical Committees of  
10 Copenhagen in Denmark (Protocol nr.: 17003845; and as part of trial H-17002476). The study  
11 recruited 4 healthy men aged 30-60 years at the Department of Pharmacy and Department of  
12 Biology, University of Copenhagen. Exclusion criteria include other use of medicine and body mass  
13 index above 30, peptic ulcers, signs of liver or kidney dysfunction. All individuals provided oral  
14 informed consent to participate in the study.

###### 15 *Collection of blood plasma and urine samples before and after APAP intake*

16 The subjects received APAP 2 × 500 mg (Panodil®, GlaxoSmithKline Aps). No subjects reported any  
17 adverse signs of taking the medication. Three baseline samples of urine (spot urine) and plasma were  
18 sampled in the morning two days and just prior to intake of APAP. Subsequently, samples were taken  
19 +1h, +2h (urine only), +4h, +6h hours after intake and in the morning of the subsequent two days  
20 (+24 and 48h) (Fig S1.). For each time point, 10-mL heparinized blood samples were collected from  
21 the antecubital vein of the non-dominant arm together with urine samples. Blood samples were  
22 centrifuged (5 min, 10,000 g) and plasma collected. Plasma and urine samples were stored at -80 °C  
23 immediately after collection.

###### 24 *Targeted analyses of APAP in blood plasma and urine*

1 APAP was analyzed using an adapted version of a method previously described (Modick et al., 2013;  
2 Modick et al., 2016). In an HPLC vial, 300  $\mu$ L ammonium acetate buffer (0.5 M, pH 5.5-6.0), 6  $\mu$ L  $\beta$ -  
3 glucuronidase type HP-2 from *Helix pomatia* (with aryl sulfatase activity; Sigma Aldrich, Steinheim,  
4 Germany), and 30  $\mu$ L internal standard (1 mg/L *N*-(4-hydroxyphenyl-2,3,5,6- $d_4$ )acetamide (APAP- $d_4$ )  
5 in water) were added to 300  $\mu$ L of the sample. After incubation at 37 °C for 3.5 h, 160  $\mu$ L 3M formic  
6 acid were added and the samples were frozen overnight. The thawed and homogenized samples  
7 were centrifuged (10 min, 1900g) and the supernatant analyzed by online-SPE-LC-ESI-MS/MS. A 1260  
8 Infinity HPLC (Agilent Technologies, Waldbronn, Germany) consisting of a G1367E autosampler with  
9 G1330B thermostat, a G1312B binary pump (LC pump) with G4225A degasser, a G1311B quaternary  
10 low pressure gradient pump (loading pump) and a G1316A thermostated column compartment with  
11 a six-port switching valve was used for the LC separation (setup depicted in (Modick et al., 2013)) and  
12 a 4500 triple quadrupole mass spectrometer (Sciex, Darmstadt, Germany) was used for detection. An  
13 Oasis HLB cartridge (2.1 x 20 mm; 25  $\mu$ m; Waters, Eschborn, Germany) was used for online SPE and  
14 an Accucore Phenyl-X (3.0 x 150 mm; 2.6  $\mu$ m; Thermo Scientific, Franklin, MA, USA) was used for the  
15 HPLC separation. Eluents were water (A) and acetonitrile (B), both containing 0.05% formic acid. 25  
16  $\mu$ L of the sample were loaded onto the SPE column at a flow of 3.75 mL/min pure eluent A. The six-  
17 port valve was switched at  $t = 2$  min to start the analyte transfer from the SPE column onto the  
18 analytical column (in back-flush) and was switched back to the loading position at  $t = 4.5$  min. From  $t$   
19 = 4.5 min to 16 min, the SPE column was flushed with 95% B for 5 min and then re-equilibrated to  
20 the starting conditions simultaneous to the analytical separation. The gradient for the analytical  
21 separation started at 15% solvent B. After 0.5 min, B was increased to 35% within 0.5 min and then  
22 increased to 45% within 3.5 min. Afterwards, B was increased to 50% within 1.5 min and then to 95%  
23 within 2 min and kept for 2.5 min. B was then returned to initial 15% within 2.5 min and kept for 3  
24 min. Detection of APAP and APAP- $d_4$  was performed with ESI-MS in positive ionization mode (time-  
25 programmed MRM). Ion source parameters were (all gases nitrogen) 35 psi curtain gas, 25 psi  
26 nebulizer and heater gas, 4.5 kV electrospray voltage, and 450 °C source temperature. Quantifier



1 mass transitions for APAP ( $t_R = 6$  min) and APAP- $d_4$  ( $t_R = 6$  min) were  $m/z$  152  $\rightarrow$  110 and  $m/z$  156  $\rightarrow$   
2 114 (collision energy (CE) 22 eV, collision cell exit potential (CXP) 7.7 V), respectively. Qualifier mass  
3 transitions were  $m/z$  152  $\rightarrow$  93 and  $m/z$  156  $\rightarrow$  97 (CE 28 eV, CXP 6.3V), respectively. The collision  
4 gas pressure setting was 5 arbitrary units and the entrance potential and declustering potential were  
5 12 V and 59 V, respectively. The limit of quantification (based on a signal-to-noise ratio of 10) was 1  
6  $\mu\text{g/L}$  APAP. Plasma samples were analyzed at least in 2-fold dilution (diluted with water). Urine  
7 concentrations were normalized to specific gravity measured using a refractometer (Atago Urine S.G.  
8 scale : 1.000 to 1.060).

9

#### 10 *Non-targeted analyses of APAP in blood plasma and urine*

##### 11 - *Chemicals*

12 The list of standards used for the identification of APAP metabolites and the 15 labelled internal  
13 standards (IS) spiked in samples for the untargeted analyses and their respective suppliers are  
14 provided in Table S1. All solvents were high-performance liquid chromatography grade, purchased  
15 from Biosolve Chime (Dieuze, France). Phree Phospholipid Removal 96-well plates and Strata-X  
16 Polymeric Reversed Phase cartridges (200 mg, 3 mL) were supplied by Phenomenex (Le Pecq,  
17 France).

18

##### 19 - *Preparation of blood plasma and urine samples*

20 Plasma samples were prepared based on the method published in David et al. (David et al., 2014)  
21 Previous studies have demonstrated that this sample preparation method developed for untargeted  
22 analysis purposes using phospholipid removal followed by polymeric reversed phase solid phase  
23 extraction extracts xenobiotics such as pharmaceuticals (including APAP), conjugated xenobiotics as  
24 well as non-polar, cationic and anionic metabolites (e.g., steroids, eicosanoids, amino acids,  
25 neurotransmitters, bile acids and lipids) from plasma samples (David et al., 2014; David et al., 2017).

1 Briefly, 400  $\mu$ L of acetonitrile with 1% formic acid (FA) was added to each blood plasma sample (100  
2  $\mu$ L). The IS mixture containing 1.5 ng of each labelled standard (see Table S1) was added to the  
3 plasma extracts. After homogenization, samples were filtered under vacuum using a 96-well sample  
4 manifold and the filtrate collected. An additional 100  $\mu$ L of acetonitrile containing 1% FA was added  
5 to the wells at the end of the filtration process to rinse the sorbent. The combined filtrates were  
6 collected and 4 mL of HPLC grade water was added to each sample. Samples were homogenized and  
7 then extracted using Strata-X cartridges which were conditioned with 4 mL methanol and  
8 equilibrated with 4 mL HPLC grade water. Samples were loaded onto the SPE cartridges. After a  
9 washing step using 2 x 3 mL of 95/5 HPLC grade water/methanol (v/v), sorbents were dried under  
10 vacuum and elution was performed with 4 mL of methanol. The eluate was evaporated to dryness,  
11 reconstituted in 15  $\mu$ L 80/20 water/acetonitrile (v/v) and stored at -80 °C until analysis.

12 Urine samples were prepared using a similar SPE protocol as the one used for the plasma. The step  
13 before SPE, i.e. removal of phospholipid and protein using the Phree plates, was omitted as urine  
14 contains lower levels of these molecules (as opposed to plasma). Previous studies have shown that  
15 methods using polymeric SPE are efficient to concentrate urine samples for untargeted analyses and  
16 extract the urinary metabolome and (xeno)metabolome (Chetwynd et al., 2015). Briefly, urine  
17 samples (500  $\mu$ L) were diluted to 4 mL of HPLC grade water, acidified with 1% formic acid and  
18 extracted using Strata-X SPE. Cartridges were conditioned with 4 mL methanol and 4 mL of HPLC  
19 grade water. Strata-X cartridges were then loaded with the 4 mL of diluted urine and washed with 2 x  
20 3 mL of 95/5 HPLC grade water/methanol (v/v). SPE phases were dried under vacuum and elution  
21 was performed with 4 mL of methanol. The eluate was evaporated to dryness, reconstituted in 50  $\mu$ L  
22 80/20 water/acetonitrile (v/v) and stored at -80 °C until analysis.

### 23 - *UHPLC-ESI-QTOFMS analyses*

24 Plasma and urine extracts were profiled using an Exon UHPLC system (AB Sciex, USA) coupled to an  
25 AB Sciex X500R Q-TOF-MS system (Sciex technologies, Canada), equipped with a DuoSpray ion  
26 source. 2  $\mu$ L of extracts were loaded and separated on an Acquity UHPLC HSS-T3 column, 1.0 mm x

1 150 mm x 1.8  $\mu$ m, maintained at 40°C (Waters Technologies, Saint Quentin, France). HPLC grade  
2 water was used as solvent A and acetonitrile as solvent B, both modified with 0.01% formic acid. The  
3 flow rate was 100  $\mu$ L/min with a gradient of 0-2.5 min from 10% to 20% B, 2.5-20 min from 20 to 30%  
4 B, 20-38 min from 30% to 45% B, 38-45 min from 45 to 100% B, 45-55 min 100% B, and equilibration  
5 to initial conditions in 5 min.

6 The Q-TOF was recalibrated automatically after each sample using an ESI positive/negative  
7 calibration solution via a calibration delivery system (CDS). As a first step, all the samples were  
8 analysed in full scan experiment (50-1100 Da) in both – and + ESI modes. The common parameters  
9 for the full scan experiment in both positive/negative ion modes were: collision energy, 10 eV;  
10 curtain gas, 35; ion source gas 1, 50; ion source gas 2, 70; temperature, 550°C; declustering potential,  
11 80 V; mass resolution of 50,000.

12 As a second step, MS/MS mass fragmentation information for chemical elucidation was obtained by  
13 further analysis of selected samples in sequential window acquisition of theoretical mass spectrum  
14 (SWATH). Selection of samples were made based on the presence of markers discriminating between  
15 the 3 groups (*baseline group*, *1-6h group* and *+1-2 days group*, see HRMS dataset section) that  
16 needed further structural MSMS confirmation. Swath data-independent acquisitions were performed  
17 in order to achieve comprehensive MS/MS sampling. The Q1 isolation window strategy was  
18 generated using the Sciex Variable Window Table from previously acquired MS data on the specific  
19 sample of interest in order to optimize window widths across the entire  $m/z$  range. SWATH  
20 experiments were performed in both – and + mode with parameters: MS1 accumulation time, 80 ms;  
21 MS2 accumulation time, 30 ms; collision energy, 35 eV; collision energy spread, 15 eV; cycle time,  
22 469 ms; mass range,  $m/z$  50–900.

23 - *Quality Control.*

24 For the untargeted analysis, one workup blank sample (i.e., extraction with HPLC grade water instead  
25 of sample) per analytical batch was prepared to monitor for background contaminants. Quality

1 control (QC) samples comprising a composite sample were prepared in order to monitor for UHPLC-  
2 ESI-TOF-MS repeatability and sensitivity during analysis of a sample run. Solvent blank samples  
3 (acetonitrile/H<sub>2</sub>O (20:80)) were also injected to ensure that there was no carryover in the UHPLC  
4 system that might affect adjacent results in analytical runs. Each batch commenced with the injection  
5 of the blank samples (workup and solvent) followed by the injection of a QC sample, and then all  
6 samples from the batch were injected randomly. As recommended, QC samples were injected within  
7 each batch periodically (i.e. every 7 sample for plasma and 5 sample for urine) to monitor the  
8 analytical sensitivity and the repeatability (n=6 QCs in plasma and n=9 QCs in urine, for each mode).  
9 To assess the UHPLC-ESI-Q-TOF-MS analytical variability during analytical runs, coefficients of  
10 variation (CV) for the peak areas were calculated for each IS in QC samples. Furthermore, the  
11 analytical variability of the plasma and urine runs was also assessed based upon the method  
12 proposed by Want et al. (Want et al., 2010). The response (i.e., the area) of each marker ( $Rt \times m/z$   
13 values) from all QC samples was normalized to the total ion signal (area) to monitor the analytical  
14 variability at the whole metabolome scale. Using this method, mean area of more than 80% of all  
15 markers present in QCs had CVs of less than 30% as recommended by Want et al. (Want et al., 2010)  
16 for metabolomics experiments (Table S4). Coefficients of variation (CVs) of the peak areas of each  
17 labelled internal standard (n=15) measured in quality controls (QCs) in plasma (n=6 QCs) and urine  
18 (n=9 QCs) were all below 20% (Table S5). To correct for extraction issues and matrix interferences,  
19 the peak area of each metabolite was adjusted to that of APAP-d4 in case of blood and to the total  
20 peak area (or sum of peak areas) in urine (Gagnebin et al., 2017) to correct mainly for urinary dilution  
21 issues.

## 22 - *HRMS dataset*

23 Mass spectra collected in full scan mode ( $m/z$  50–1100) and spectral peaks were preprocessed (i.e.,  
24 deconvolution, alignment, peak picking) using both the open source R package XCMS (Smith et al.,  
25 2006) and vendor software MarkerView 1.3.1 (AB, Sciex) to create separate aggregate datasets from  
26 all sample files in which the MS features were binned into retention time ( $Rt$ )  $\times$   $m/z$  values. For

1 XCMS, the raw data files were first converted to 64 bit .mzML (full scan) using MSConvert from  
2 ProteoWizard (Adusumilli and Mallick, 2017).

3 The peak tables obtained with XCMS were used for multivariate and univariate analyses in an R  
4 environment (R version 3.6.0) in order to identify APAP metabolites after APAP exposure (see Table  
5 S2 for parameters used). Principal component analyses (PCA) were performed as a first step to  
6 examine QC clustering, sample separation and identify any analytical or biological outliers (See Fig.  
7 S2 and S3). Sample groups were then defined as follows in order to perform Sparse Partial Least  
8 Squares Discriminant Analyses (sPLS-DA) models: *baseline group* = samples collected two days and  
9 just prior to intake of APAP, *1-6h group* = samples collected +1, +2, +4, +6 hours after intake and *+1-2*  
10 *days group* = samples collected in the morning the subsequent two days. sPLS-DA was performed  
11 with mixOmics R package (version 6.8.5) in the mode regression (Rohart et al., 2017) (See Fig. S4 and  
12 S5). Besides multivariate analyses, univariate analyses were performed to compare fold changes of  
13 markers between the three different groups with the mixOmics R package. A corresponding p-value  
14 was calculated with the multtest R package using Unpaired Student's t-tests, with an Adaptive  
15 Benjamini and Hochberg (ABH) correction for multiple comparisons to identify markers  
16 discriminations between groups. All markers having p-value < 0.01 were selected for further  
17 tentative annotation process.

18 Discriminating markers between the three groups identified through multi- and univariate analyses  
19 were first screened using a list of known APAP metabolites. The suspect list was build using  
20 information already available in the literature and using *in silico* software tools that predicts small  
21 molecule metabolism in mammals (e.g., BioTransformer (Djoumbou-Feunang et al., 2019a)).  
22 Identities of these expected APAP metabolites were determined from accurate mass, isotopic fit,  
23 fragmentation data obtained from SWATH acquisition and from comparison with standard  
24 compounds when available or spectra available in online libraries or the literature. In order to  
25 provide confidence in metabolite identification, we supply confidence levels based on

1 recommendations made by Schymanski et al. (Schymanski et al., 2014) (see Supp. Table S6). The  
2 structural identities of unknown discriminating markers were determined from their accurate mass,  
3 isotopic fit, fragmentation data obtained from SWATH acquisition. These parameters were compared  
4 with those from online libraries such as PubChem (Kim et al., 2019), ChemSpider (Pence and  
5 Williams, 2010), KEGG (Kanehisa, 2002), HMDB (Wishart et al., 2018b), Metlin (Guijas et al., 2018),  
6 T3DB (Wishart et al., 2015), MassBank (Horai et al., 2010) or DrugBank (Wishart et al., 2018a). When  
7 no experimental spectra were available, MS/MS fragmentation patterns of individual markers were  
8 collected and annotation was based on online software such as MetFrag (Ruttkies et al., 2016) and  
9 CFM-ID (Djoumbou-Feunang et al., 2019b)) which allow to perform *in silico* fragmentation of  
10 candidate molecules from different databases (e.g., PubChem) and search for matched against mass  
11 to charge values. When possible, chemical identity was confirmed from accurate mass, isotopic fit  
12 and fragmentation data obtained from standard compounds (highest level of confidence). In the end,  
13 only annotations with a confidence level higher than 2b (i.e., based on MS/MS match with  
14 experimental or *in silico* MS/MS spectra) were reported.

15 - *Accurate integration of identified and annotated markers*

16 Independent peak integration and normalization were carried out to validate the significance of the  
17 discriminated metabolites between groups. All the markers identified were manually re-integrated  
18 using the Sciex OS Analytics tool. The integrated peak area of individual markers was normalized to  
19 APAP-d4 for plasma or to a corrective factor based on the total peak area measured with MarkerView  
20 for urine (this corrective factor was calculated by dividing the total peak area of each sample to that  
21 of a reference sample). Prism 8 software (GraphPad Software) was used to generate plots.

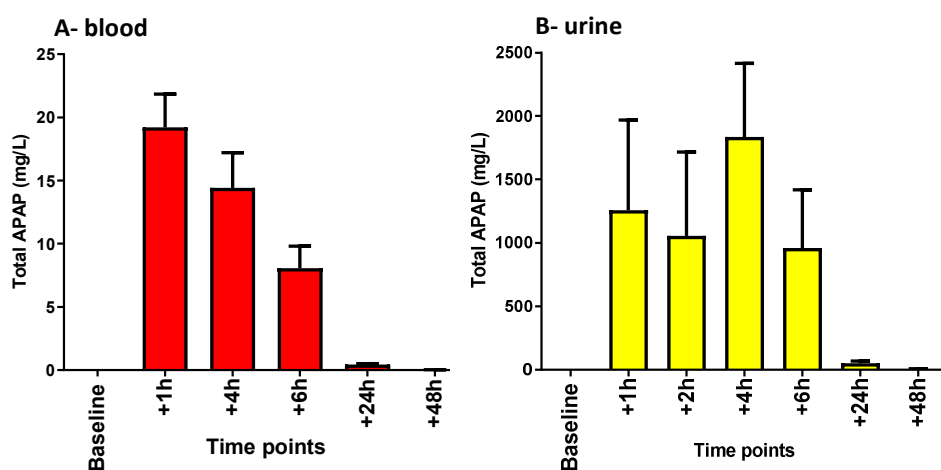
22

23 **RESULTS AND DISCUSSION**

24 *Targeted analyses of APAP in blood plasma and urine*

1 Results with targeted analyses confirmed the presence of APAP in urine ( $0.107 \pm 0.025$  mg/L, mean  $\pm$   
2 SEM, min=0.002 mg/L, max=0.200 mg/L; n =12) before the intentional APAP dose, similar to  
3 concentrations previously observed in the German (Modick et al., 2014) and the Danish populations  
4 (Nielsen et al., 2015). As illustrated in Fig 1, the peak APAP concentration in blood plasma was  
5 observed already one hour after APAP intake (mean concentration of 19.2 mg/L) in the range of  
6 plasma therapeutic concentrations previously measured (5-25 mg/L) (Schulz et al., 2012). In urine,  
7 the peak APAP concentration was observed after 4 h (mean concentration of 1.83 g/L). After 24 h  
8 and 48 h, median urinary APAP concentrations were 2.7% (mean concentration of 49.6 mg/L) and  
9 0.3% (median concentration of 5.6 mg/L) of the maximum mean urinary concentrations, respectively.  
10 The mean APAP urinary concentrations observed 24-48 h after APAP intake were about 50-450 fold  
11 higher than the one observed before APAP intake, but overlap with the environmental APAP  
12 concentrations previously observed in urine from the general population among non-users and non-  
13 smokers from 0.95 to 580.4 mg/L, mean=4.1 mg/L (Modick et al., 2014), confirming that, in some  
14 cases, pharmaceutical APAP use cannot be distinguished from the environmental exposure after 24 h  
15 using present standard targeted methods.

16



17

18 **Fig. 1.** “Total” APAP concentrations (free APAP, APAP glucuronide and APAP sulfate) after enzymatic  
19 deconjugation using LC-MS/MS in (A) blood plasma (mg/L, mean  $\pm$  SEM) and (B) urine (mg/L, mean  $\pm$  SEM) of

1 the 4 men before APAP intake (baseline, n=12) and at different time points after intake. Urine concentrations  
2 are normalized to specific gravity.

### 3 *Detection of new APAP metabolites in humans using HRMS-based non-targeted analyses*

4 To gain a deeper insight into APAP metabolism, we next analyzed samples from the longitudinal  
5 exposure with a non-targeted HRMS-based method. Discriminating markers between the *baseline*  
6 group (samples collected two days and just prior APAP intake), the *+1-6h* group (samples collected  
7 from 1h up to 6h after APAP intake), and the *+1-2 days* group (samples collected in the morning of  
8 the subsequent two days after APAP intake) were identified through multi- and univariate analyses.  
9 In total, APAP and 14 of its (proposed or confirmed – see below) metabolites could be annotated and  
10 identified in blood and urine after APAP intake with confidence levels ranging from 2a-2b (annotation  
11 based on MS/MS match with experimental or *in silico* MS/MS spectrum) to 1 (confirmation of  
12 identification with a standard) according to Schymanski et al. (Schymanski et al., 2014). The list of all  
13 APAP metabolites detected in human blood and urine, their respective confidence levels, as well as  
14 the metabolic pathway involved are reported in Table 1 (see Table S6 for more information on  
15 criteria used for the annotation/identification including the list of MS/MS fragments).

16 **Table 1.** List of APAP and its metabolites detected in human blood and urine at different time points after APAP  
17 intake using high-resolution mass spectrometry. The highest level of evidence used for the annotation and  
18 identification of APAP metabolites, their respective pathway and the enzymes involved as well as previous  
19 detections in human or mammals are reported.



List of APAP/metabolites and associated pathways	Formula	Confid. Level <sup>1</sup>	Highest level of evidence for identification/annotation	Main enzymes involved	Reported in humans	Reported in rodents/dogs
<b>Parent</b>						
APAP	C8H9NO2	1	Rt and MSMS match with std		yes	yes
<b>Direct phase II reactions</b>						
APAP-S	C8H9NO5S	2a	MSMS match with experimental MSMS spectra from a library <sup>2</sup>	STs	yes	yes
APAP-Glu	C14H17NO8	1	Rt and MSMS match with std	UDPGTs	yes	yes
<b>Catechol pathway</b>						
3-OH-APAP	C8H9NO3	1	Rt and MSMS match with std	CYP450	yes	yes
3-OH-APAP-S	C8H9NO6S	2a	MSMS match with experimental MSMS spectra from a library <sup>2</sup>	+STs +UDPGTs	yes	yes
3-OCH <sub>3</sub> -APAP-Glu	C15H19NO9	2a	MSMS match with experimental MSMS spectra from a library <sup>2</sup>		yes	yes
<b>Mercapturic acid pathway</b>						
APAP-Cys	C11H14N2O4S	1	Rt and MSMS match with std	CYP450 (for NAPQI)	yes	yes
NAC-APAP	C13H16N2O5S	1	Rt and MSMS match with std	+GSTs	yes	yes
NAC-O-APAP	C13H16N2O6S	2b	MSMS match with <i>in silico</i> MSMS spectra <sup>3</sup>	+GGTs, CGDs +NATs	no	no
<b>Thiomethyl shunt pathway</b>						
SH-APAP-Glu	C14H17NO8S	2b	MSMS match with <i>in silico</i> MSMS spectra <sup>3</sup>	After mercapturate pathway:	no	no
S-CH <sub>3</sub> -APAP	C9H11NO2S	1	Rt and MSMS match with std		yes	yes
S-CH <sub>3</sub> -APAP-S	C9H11NO5S2	2b	MSMS match with experimental MSMS spectra (literature) <sup>4</sup>	+ CS lyases + SMTs	no	yes
S-CH <sub>3</sub> -APAP-Glu	C15H19NO8S	2b	MSMS match with <i>in silico</i> MSMS spectra <sup>3</sup>	+ STs + UDPGTs	no	yes
SO-CH <sub>3</sub> -APAP-S	C9H11NO6S2	2b	MSMS match with <i>in silico</i> MSMS spectra <sup>3</sup>		no	only as unconjugated
SO-CH <sub>3</sub> -APAP-Glu	C15H19NO9S	2b	MSMS match with <i>in silico</i> MSMS spectra <sup>3</sup>		no	only as unconjugated

1

2 <sup>1</sup> Schymanski et al., 2014; <sup>2</sup> Metlin, HMDB; <sup>3</sup> MetFrag and CFM-ID; <sup>4</sup> Patterson et al., 2013. STs=

3 sulfotransferases; UDPGTs= uridine diphosphoglucuronyltransferases; GSTs= glutathione S-transferases; GGTs=

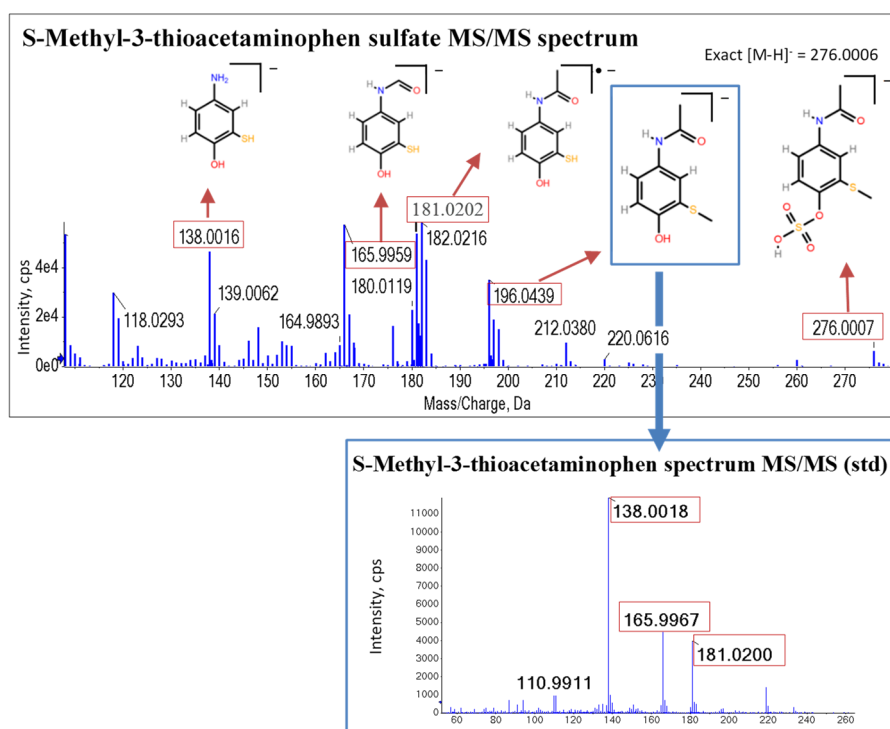
4 gamma glutamyltransferases, CGDs= cysteinylglycine dipeptidases; NATs= N-acetyltransferases; CS lyases =

5 Cysteine S-conjugate β-lyases; SMTs= S-methyl-transferases

6 Based on relative peak areas, the main APAP metabolites detected in blood and urine samples  
7 collected +1-6h after APAP intake include direct phase II glucuronide (APAP-Glu) and sulfate (APAP-S)  
8 conjugates. APAP-Glu and APAP-S are formed by direct glucuronidation and sulfation of APAP in the  
9 liver through the action of sulfotransferases (ST) and uridine diphosphoglucuronyltransferase  
10 (UDPGTs) (Mazaleuskaya et al., 2015). We also detected in this group glutathione-derived APAP  
11 metabolites originating from the phase I reactive NAPQI, i.e., APAP-Cys and NAC-APAP. APAP is  
12 activated in the liver to form the toxic NAPQI under the mediation of CYP450 enzymes which is then  
13 almost immediately detoxified in the liver through the action of the glutathione transferases  
14 (Bessemers and Vermeulen, 2001). Glutathione conjugates are then biotransformed in the liver as

1 APAP-Cys and then NAC-APAP through the mercapturic acid pathway by the sequential action of the  
2  $\gamma$ -glutamyltransferases, dipeptidases, and cysteine *S*-conjugate *N*-acetyltransferase (Hanna and  
3 Anders, 2019). Finally, we also detected in this *+1-6h* group catechol APAP metabolites originating  
4 from another phase I oxidation pathway (i.e., 3-OH-APAP and 3-OCH<sub>3</sub>-APAP present as non-  
5 conjugated and conjugated forms).

6 Of the 14 metabolites, we also annotated conjugated forms of *S*-methyl-3-thioacetaminophen (*S*-  
7 CH<sub>3</sub>-APAP-*S* and *S*-CH<sub>3</sub>-APAP-*Glu*) and *S*-methyl-3-thioacetaminophen sulphoxide (SO-CH<sub>3</sub>-APAP-*S*  
8 and SO-CH<sub>3</sub>-APAP-*Glu*) up to now unreported in humans as conjugated. These 4 conjugated  
9 metabolites had previously only been reported in rodents (rat and hamster) and dogs (albeit non-  
10 conjugated in case of SO-CH<sub>3</sub>-APAP-*S* and SO-CH<sub>3</sub>-APAP-*Glu*; i.e., SO-CH<sub>3</sub>-APAP) (Gemborys and  
11 Mudge, 1981; Hart et al., 1982; Mikov et al., 1988). The two metabolites NAC-O-APAP and SH-APAP-  
12 *Glu* have not at all been detected before in any species to the best of our knowledge. Except for NAC-  
13 O-APAP, these conjugated thiomethyl metabolites (i.e., *S*-CH<sub>3</sub>-APAP-*S*, *S*-CH<sub>3</sub>-APAP-*Glu*, SO-CH<sub>3</sub>-  
14 APAP-*S* and SO-CH<sub>3</sub>-APAP-*Glu* metabolites) were mainly detected in samples collected *+1-2 days*  
15 after APAP intake.



1

2 **Fig.2.** Experimental MS/MS spectrum of S-Methyl-3-thioacetaminophen sulfate from a urine sample (+24h time

3 point) after APAP exposure and MS/MS spectrum of the standard of S-Methyl-3-thioacetaminophen. MS/MS

4 mass fragmentation information was obtained in SWATH mode using an UHPLC-ESI-QTOF-MS in –ESI mode. *In*

5 *silico* fragmentation software (i.e., MetFrag and CFM-ID) were utilized for computer assisted identification for

6 S-Methyl-3-thioacetaminophen sulfate. Further confirmation of experimental MS/MS fragments could be

7 obtained by injecting the commercially available standard of S-CH<sub>3</sub>-APAP.

8 *In silico* fragmentation software such as MetFrag (Ruttkies et al., 2016) and CFM-ID (Djombou-

9 Feunang et al., 2019b) were utilized for computer assisted annotation of S-CH<sub>3</sub>-APAP-S and SO-CH<sub>3</sub>-

10 APAP-S since many potential candidates were matching the matching the accurate mass of these

11 marker ions within PubChem (e.g., 1337 candidates for m/z=276.004 in –ESI mode [M-H]<sup>-</sup>; 5 ppm

12 mass tolerance). Further confirmation of the S-CH<sub>3</sub>-APAP-S annotation were obtained by comparing

13 its experimental MS/MS fragments with those of its non-conjugated form (S-CH<sub>3</sub>-APAP), which was

14 obtained by injecting the S-CH<sub>3</sub>-APAP standard in SWATH mode (Fig. 2). Moreover, the MS/MS

15 fragments of S-CH<sub>3</sub>-APAP-S we report are matching those observed experimentally in mice after

16 APAP exposure (Patterson et al., 2013). The other marker with an m/z of 291.9945 in –ESI mode ([M-

1 H<sup>-</sup>) could be annotated as S-CH<sub>3</sub>-APAP sulfoxide derivative, i.e., SO-CH<sub>3</sub>-APAP-S (see Fig. S6 for  
2 MS/MS spectra). Although standards or MS/MS spectra are currently unavailable for most of these  
3 metabolites, a high level of confidence could be reached (Schymanski et al., 2014; Sumner et al.,  
4 2007) given that a match was observed with the MS/MS profile of the standard for the unconjugated  
5 S-CH<sub>3</sub>-APAP and that the metabolites are related to the same pathway of elimination of thio  
6 metabolites.

7

### 8 *Relevance of thiomethyl metabolites for monitoring APAP pharmaceutical use*

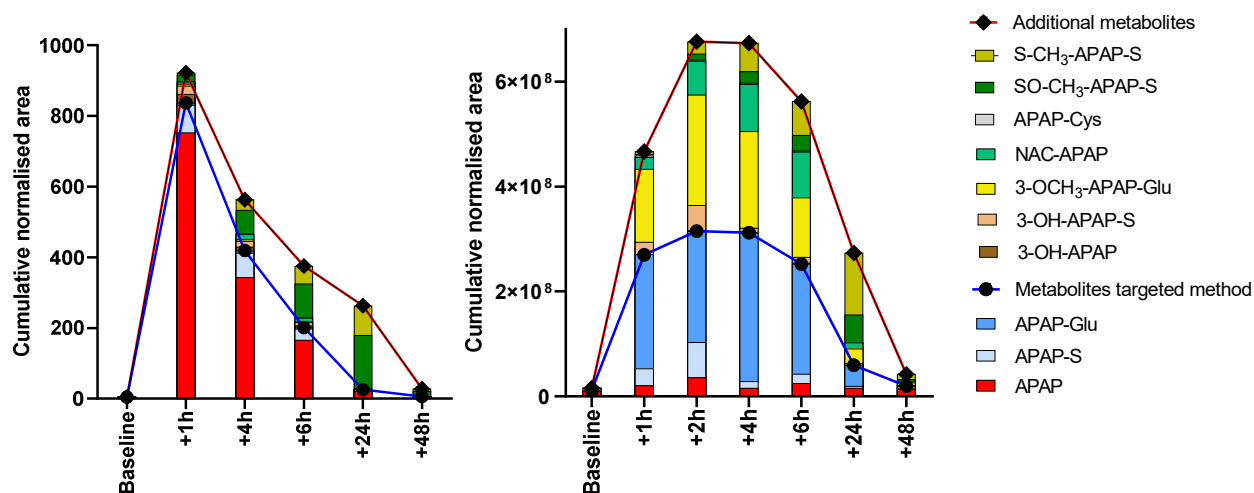
9 To understand the relevance of the 4 conjugated thiomethyl metabolites (S-CH<sub>3</sub>-APAP-S, S-CH<sub>3</sub>-APAP-  
10 Glu, SO-CH<sub>3</sub>-APAP-S and SO-CH<sub>3</sub>-APAP-Glu) and the two previously unreported metabolites NAC-O-  
11 APAP and SH-APAP-Glu metabolites to improve human biomonitoring of APAP , we next investigated  
12 the relative contributions of APAP metabolites in urine and plasma based on their analytical  
13 responses (normalized peak areas) for each time point. We also compared the analytical responses of  
14 free APAP and its phase II conjugates, conventionally used in standard APAP biomonitoring methods,  
15 to those of catechol and glutathione-derived APAP metabolites. Although these HRMS-based data  
16 are not representative of the importance of each metabolite in APAP metabolism in terms of  
17 quantity excreted, they do provide valuable information regarding the most sensitive metabolites (in  
18 respect to their ionization efficiency) to be used for optimizing APAP monitoring in humans. The  
19 relative contributions based on normalized peak area of APAP metabolites are presented in Fig.3 for  
20 both blood and urine.

21

22

23

24



1  
2 **Fig. 3.** Analytical responses (represented as cumulative normalised peak areas) of APAP metabolites classically  
3 used for targeted methods (i.e., free APAP, APAP-Glu and APAP-S) and the other metabolites detected using  
4 the non-targeted analyses in blood (A) and urine (B) of the 4 men. APAP and its metabolites were manually re-  
5 integrated using the Sciex OS Analytics tool. The integrated peak area of individual markers was normalized to  
6 APAP-d4 for plasma or with a corrective factor based on the total peak area for urine.

7 Of the 6 metabolites previously unreported in humans, only the sulfate thiomethyl metabolites (i.e.  
8 S-CH<sub>3</sub>-APAP-S and SO-CH<sub>3</sub>-APAP-S) present significant analytical responses and therefore potential to  
9 improve APAP monitoring. Relative contributions of S-CH<sub>3</sub>-APAP-Glu, SO-CH<sub>3</sub>-APAP-Glu, NAC-O-APAP  
10 and SH-APAP-Glu are not reported on Fig. 3 as they were <1% for all time points after APAP intake. In  
11 particular, we observed that S-CH<sub>3</sub>-APAP-S and SO-CH<sub>3</sub>-APAP-S are major metabolites for the 24h and  
12 48h time points in blood and urine while the contributions of these S-CH<sub>3</sub>-APAP-S and SO-CH<sub>3</sub>-APAP-S  
13 metabolites are minor before APAP intake (baseline).

14 More specifically, the relative contribution of the parent APAP was major in blood for the first time  
15 points after APAP intake (relative contribution of 44-82% before 24h) while these of other APAP  
16 metabolites such as phase II APAP-S, catechol APAP (OH-APAP and OH-APAP-S), or NAC-APAP were  
17 all comprised below 12% for the same time points. Relative contributions of S-CH<sub>3</sub>-APAP-S and SO-  
18 CH<sub>3</sub>-APAP-S increased overtime after APAP intake, finally becoming dominant for the 24h and 48h  
19 time points (i.e., 90% and 78% at 24h and 48h, respectively, for the sum of both metabolites).

1 In urine, the metabolites conventionally used for the monitoring of APAP using targeted approach,  
2 i.e. free APAP and the phase II conjugates (APAP-S and APAP-Glu) contributed to 45-58% of the  
3 analytical response for the time points comprised between +1h and 6h. APAP-Glu was the major  
4 metabolite for these time points (relative contribution of 31-46% overall). The other catechol or  
5 glutathione-derived metabolites and conjugated thiomethyl metabolites contributed altogether to  
6 the remaining 42-55% of the analytical response from 1h up to 6h after APAP intake. For these 1-6h  
7 time points, 3-OCH<sub>3</sub>-APAP-Glu was the major metabolite among these metabolites (relative  
8 contribution of 20-31% overall), followed by NAC-APAP (5-15 % overall), S-CH<sub>3</sub>-APAP-S (1-11%  
9 overall) and SO-CH<sub>3</sub>-APAP-S (0.6 -5% overall). As observed in blood, S-CH<sub>3</sub>-APAP-S and SO-CH<sub>3</sub>-APAP-S  
10 were major metabolites for the 24h and 48h time points (relative contribution for the sum of both  
11 metabolites of 36-62% between 24h and 48h).

12 As mentioned earlier, the relative contributions of APAP metabolites reported here are not fully  
13 representative of the importance of each metabolite in APAP metabolism in terms of quantity  
14 excreted. APAP is known to be extensively metabolized in the liver and based on literature reviews  
15 on APAP pharmacokinetics, it is often considered that free APAP and direct phase II conjugates  
16 represent between 65-85% of the quantity excreted (mainly as APAP-Glu) while the other catechol  
17 and glutathione-derived metabolites can represent up to 20% together of the quantity excreted  
18 (Bessems and Vermeulen, 2001; Mazaleuskaya et al., 2015). However, based on the high analytical  
19 response we observed here for the conjugated catechol 3-OCH<sub>3</sub>-APAP-Glu, we show that this  
20 metabolite would be a good candidate to improve the analytical sensitivity of targeted methods  
21 based on LC-ESI-MS/MS, which is the standard platform used for APAP monitoring.

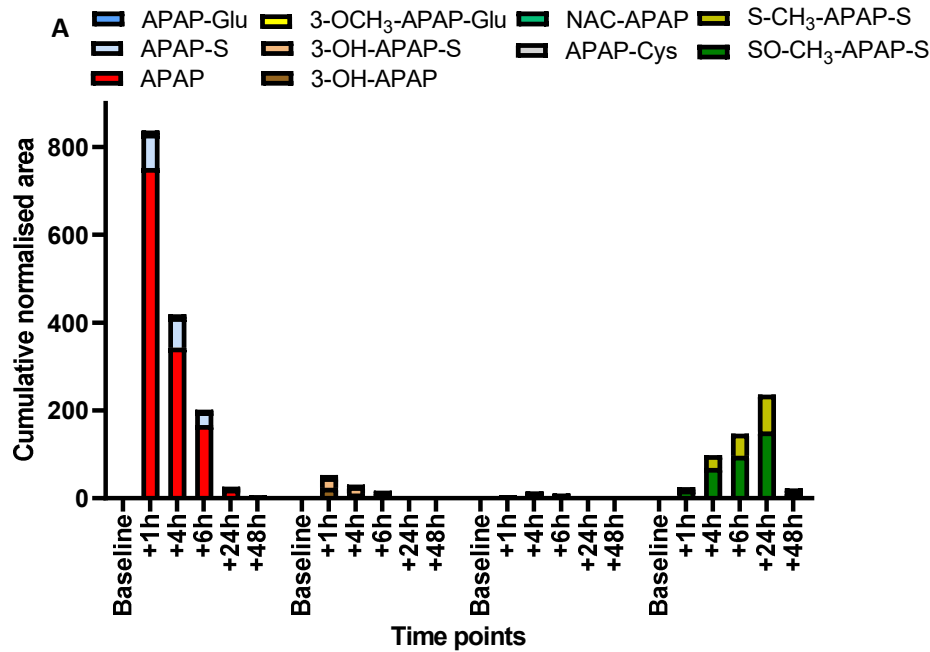
22 Background APAP exposure levels did not seem to be accompanied by significant amounts of the  
23 conjugated thiomethyl metabolites, while after pharmaceutical use (high exposure) scenario, they  
24 could be determined sensitively more than 48h post exposure, suggesting that S-CH<sub>3</sub>-APAP-S and SO-  
25 CH<sub>3</sub>-APAP-S have great potential to retrospectively assess pharmaceutical use of APAP in humans.

1 Importantly, S-CH<sub>3</sub>-APAP-S and SO-CH<sub>3</sub>-APAP-S present similar frequency of distribution in the four  
2 individuals compared to APAP metabolites such as APAP-Glu and 3-OCH<sub>3</sub>-APAP-Glu that show the  
3 highest analytical sensitivity (see Figure S7). They could be detected in all individuals (in both blood  
4 and urine) with coefficients of variation (CV) ranging from 54 to 74% in urine at time points close to  
5 their peak times. These CVs are similar to those of APAP-Glu and 3-OCH<sub>3</sub>-APAP-Glu (from 18 to 70%),  
6 suggesting that the use of S-CH<sub>3</sub>-APAP-S and SO-CH<sub>3</sub>-APAP-S as relevant markers of APAP intake in  
7 human could be generalized.

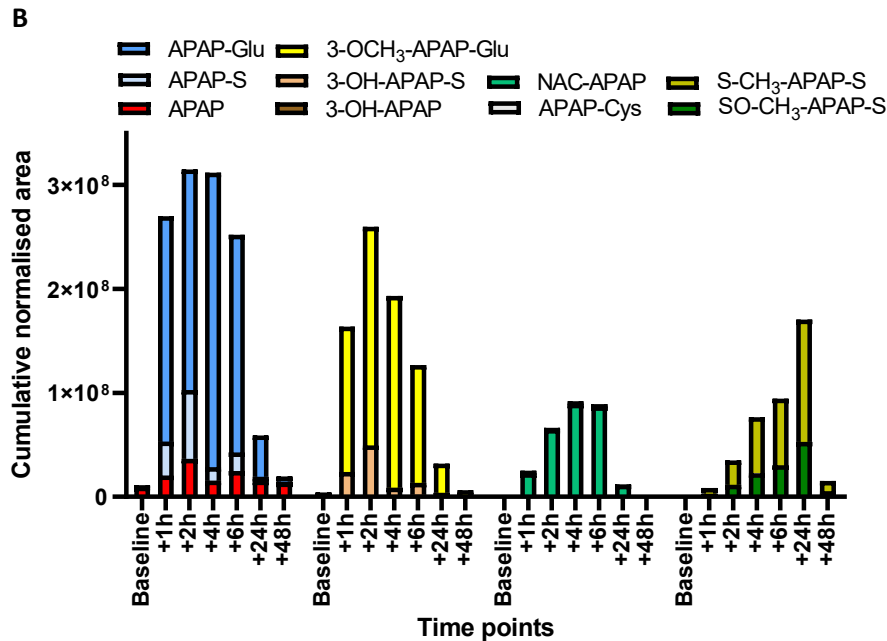
#### 8 *The conjugated thiomethyl metabolites and the thiomethyl shunt pathway*

9 We next studied the kinetics of formation of individual metabolites by comparing their normalized  
10 abundance in plasma and urine for each time point before and after APAP intake. The kinetics of  
11 formation of free APAP, phase II metabolites (APAP-Glu and APAP-S), catechol metabolites (3-OCH<sub>3</sub>-  
12 APAP-Glu, OH-APAP-S and OH-APAP), glutathione derived metabolites (NAC-APAP and Cyst-APAP)  
13 and thiomethyl metabolites (S-CH<sub>3</sub>-APAP-S and SO-CH<sub>3</sub>-APAP-S) in both blood and urine are  
14 presented in Fig. 4.

15 Similarly to the results obtained with the targeted methods, we observed that APAP was absorbed  
16 quickly in the blood and reached the peak blood concentrations within 60 minutes after ingestion, as  
17 previously observed (Mazaleuskaya et al., 2015). The APAP signal had decreased to less than 50% 4h  
18 after intake before reaching basal levels after 24-48h. Similar kinetics of formation were observed in  
19 blood for the minor APAP catechol metabolites (peak time at 1h) while NAC-APAP peaked at 4h  
20 instead, which could be explained by the fact that NAC-APAP is formed after a higher number of  
21 successive reactions involving phase I reactions, glutathione conjugation and enzyme reactions from  
22 the mercapturic acid pathway. Interestingly, S-CH<sub>3</sub>-APAP-S and SO-CH<sub>3</sub>-APAP-S metabolites in general  
23 showed delayed appearance with a peak time at 24h in blood plasma.



1



2

3 **Fig. 4.** Kinetics of formation of free APAP, phase II metabolites (APAP-Glu and APAP-S), catechol metabolites (3-  
 4 OCH<sub>3</sub>-APAP-Glu, OH-APAP-S and OH-APAP), glutathione derived metabolites (NAC-APAP and APAP-Cys) and  
 5 thiomethyl metabolites (S-CH<sub>3</sub>-APAP-S and SO-CH<sub>3</sub>-APAP-S) detected using the non-targeted screening based  
 6 on UHPLC-ESI-QTOF-MS analyses in **(A)** blood plasma and **(B)** urine of the 4 men before intake and at different  
 7 time points after intake. No significant shift (i.e. below 20%) in analytical sensitivity was observed during the  
 8 batch to make this time point comparison for individual metabolites. APAP and its metabolites were manually

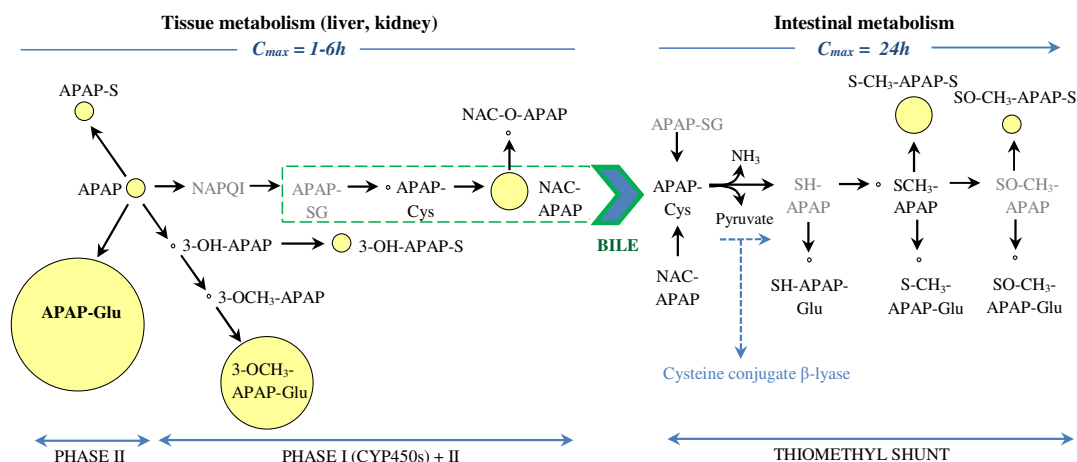


1 re-integrated using the Sciex OS Analytics tool. The integrated peak area of individual markers was normalized  
2 to APAP-d4 for plasma or with a corrective factor based on the total peak area for urine.

3 In urine, free APAP, phase II metabolite (APAP-S) and catechol metabolites (3-OCH<sub>3</sub>-APAP-Glu, OH-  
4 APAP-S and OH-APAP), peaked at 2h. This is different from the targeted results that showed that  
5 “total APAP” measured as free APAP, APAP-Glu and APAP-S after enzymatic conjugation peaked at 4h  
6 in urine instead (even though APAP-Glu taken separately also peaked at 4h with the non-targeted  
7 analyses) . However, direct comparison of quantitative data from targeted methods and semi-  
8 quantitative data from HRMS-based methods can be difficult because of the lack of specific  
9 correction with proper labelled internal standards. NAC-APAP peaked after the direct phase II  
10 conjugates and the catechol metabolites (peak time is at 4h), probably because of the higher number  
11 of successive reactions to form the mercapturic acid as mentioned earlier. Like in blood, S-CH<sub>3</sub>-APAP-  
12 S and SO-CH<sub>3</sub>-APAP-S metabolites in general showed delayed appearance compared with direct  
13 phase II conjugates, catechol metabolites and glutathione-derived metabolites that peaked in the 1h-  
14 4h window.

15 This delayed appearance suggests that the formation of S-CH<sub>3</sub>-APAP-S and SO-CH<sub>3</sub>-APAP-S was  
16 limited by prior biological steps as opposed to the direct excretion for other metabolites. A similar lag  
17 time has been observed in enterohepatic circulation due to the intestinal transit period of  
18 metabolites to sites of biotransformation (Roberts et al., 2002). Moreover, the biotransformation  
19 that leads to the formation of thiomethyl metabolites have been shown to occur in rodents via the  
20 enterohepatic circulation and biliary excretion of the glutathione-derived conjugates (i.e., APAP-Cys  
21 and NAC-APAP) into the intestine with subsequent microbiotic transformation (Gemborys and  
22 Mudge, 1981) (Fig. 5). This transformation includes activity of the cysteine S-conjugate β-lyase and  
23 subsequent methylation involving an active form of methionine (Cooper et al., 2011; Gemborys and  
24 Mudge, 1981). Therefore, our data strongly suggests that a thiomethyl shunt pathway (Cooper et al.,  
25 2011) that results in formation of the thiomethyl metabolites is also present in humans. In

1 agreement with that, the cysteine conjugate beta-lyase was already previously detected in a majority  
 2 of gastrointestinal bacteria tested (Larsen, 1985).



3  
 4 **Fig. 5.** Revisited APAP metabolism in human including the thiomethyl shunt and the role of cysteine conjugate  
 5 beta-lyase from the non-targeted screening results. APAP metabolites in grey are known precursors but not  
 6 detected during this experiment because of their lability or lower levels.

7 Hence, our results show that the conjugated thiomethyl metabolites S-CH<sub>3</sub>-APAP-S and SO-CH<sub>3</sub>-APAP-  
 8 S have the potential to improve APAP biomonitoring in humans since their delayed elimination peaks  
 9 could extend the window of exposure and thus potentially decrease underestimation or  
 10 misclassification in epidemiological studies when sampling is performed >24h after intake.

### 11 Conclusion

12 Reliable biomonitoring methods are essential for proper risk assessment. Estimations of exposure in  
 13 most existing epidemiological data of APAP have limitations due to potential recall bias or reliance on  
 14 standard analytical methods for exposure assessment which include metabolites that capture only  
 15 partially the exposure and/or are too rapidly eliminated. Our data provide a proof-of-concept for  
 16 HRMS-based non-targeted analyses as a valuable addition to the tool set for the identification of  
 17 metabolites suitable as exposure biomarkers, complementing HRMS-based suspect screening  
 18 approaches (e.g., (Lessmann et al., 2018)) and traditional approaches (e.g., (Bury et al., 2019)), and  
 19 thus contributing to the optimization of current standard methods. The findings based on non-

1 targeted analyses after APAP intake suggest that thiomethyl sulfate APAP metabolites and 3-OCH<sub>3</sub>-  
2 APAP-Glu should be included in future biomonitoring methods for several reasons. First, the  
3 conjugated thiomethyl metabolites have later peak levels and therefore extend the window of  
4 exposure decreasing underestimation. Secondly, the data suggest that they provide biomarkers of  
5 comparable sensitivity as free APAP and its phase II conjugates. Thirdly, the thiomethyl sulfate APAP  
6 metabolites provide information regarding metabolic pathways worth of interest from a toxicological  
7 point of view since they are derived from the toxic NAPQI metabolites.

8 We acknowledge that non-targeted analyses present limitations inherent to the production of semi-  
9 quantitative data and therefore the estimates we provide here will require further evaluation based  
10 on quantitative measurements and authentic standards. Nevertheless, our quality control data,  
11 showing no drift in analytical sensitivity during our batch analyses, provide confidence for the sample  
12 to sample comparison made to study the kinetics of appearance of individual metabolites at different  
13 time points. The comparison of the relative contributions of APAP metabolites based on their  
14 analytical responses is relevant to determine which metabolites can be used to optimize standard  
15 targeted methods given that similar platforms (LC-MS) and ion sources (i.e. electrospray ion sources)  
16 are utilized for the APAP targeted approach. The standard APAP biomonitoring methods include a  
17 deconjugation step using glucuronidases and sulfates. Hence, standard APAP biomonitoring methods  
18 could already be upgraded by including 3-OCH<sub>3</sub>-APAP and S-CH<sub>3</sub>-APAP metabolites as these standards  
19 are already commercially available. We therefore believe that the limitations in quantitative  
20 information value should not overshadow the importance of the identification of the thiomethyl  
21 conjugates and their potential to improve the monitoring of non-persistent chemicals such as APAP.

22 The role of the mercapturate pathway and the cysteine S-conjugate beta-lyases in the metabolism of  
23 drugs (e.g., methazolamide, cisplatin) have been already demonstrated in mammals (Cooper et  
24 al., 2011). Furthermore, the cysteine S-conjugate beta-lyases can play an important key role in the  
25 bioactivation of halogenated alkenes (some of which are environmental contaminants produced on

1 an industrial scale), and if the sulfur-containing fragment is reactive, the parent cysteine S-conjugate  
2 may be toxic, particularly to kidney mitochondria (Cooper et al., 2011; Cooper and Pinto, 2006).  
3 Despite its biological importance, there are surprisingly few data regarding identities of xenobiotics  
4 detoxified using the mercapturate and thiomethyl shunt pathway. Determining to which extent this  
5 happens could improve biomonitoring analytical methods by including more relevant metabolites  
6 and thus reduce potential serious underestimations for the reason stated above for APAP. This effort  
7 will require a coordinated approach between experts working with both targeted and untargeted  
8 approaches and the synthesis of standards for individual chemicals and their metabolites for  
9 accurate measurements. Analytical methods based on HRMS are still under development and are not  
10 mature enough to replace targeted methods in large biomonitoring programs where accurate  
11 quantitative data are needed. However, we advocate for their use as discovery-based approach, as  
12 demonstrated here, to update targeted methods with the best metabolites in order to provide the  
13 most comprehensive view of the exposure for proper risk assessment for APAP and other similar  
14 non-persistent chemicals.

15

16

#### 17 **Author's contribution**

18 AD contributed to the study design, data collection, data analysis, data interpretation, figures and  
19 tables editing, drafting and text revision; JC contributed to the data collection, data analysis, figures  
20 and tables editing, text revision; TL contributed to the data analysis, text revision; RAS contributed to  
21 the data collection, data analysis, text revision; MDD contributed to the study design, sample  
22 collection, text revision; BS contributed to the study design, sample collection; DB contributed to  
23 data collection, data analysis, data interpretation, and text revision; HMK contributed to data  
24 analysis, data interpretation, figures and tables editing, drafting and text revision; BJ contributed to

1 figures and tables editing, drafting and text revision; DMK contributed to the study design, data  
2 collection, data analysis, data interpretation, figures and tables editing, drafting and text revision.

### 3 **Acknowledgment**

4 We declare no competing interests. We thank Shanna Swan for her editorial comments and Romain  
5 Letourneur and Claudia Pälme for technical assistance. The study was supported by the Candys  
6 Foundation and a research chair of excellence (2016-52/IdeX University of Sorbonne Paris Cité)  
7 awarded to AD.

### 8 **Reference**

- 9 Adusumilli, R., Mallick, P., 2017. Data Conversion with ProteoWizard msConvert. *Methods Mol Biol.*  
10 1550, 339-368.
- 11 Albert, O., Desdoits-Lethimonier, C., Lesne, L., Legrand, A., Guille, F., Bensalah, K., Dejuccq-Rainsford,  
12 N., Jegou, B., 2013. Paracetamol, aspirin and indomethacin display endocrine disrupting  
13 properties in the adult human testis in vitro. *Hum Reprod.* 28, 1890-8.
- 14 Bessems, J.G., Vermeulen, N.P., 2001. Paracetamol (acetaminophen)-induced toxicity: molecular and  
15 biochemical mechanisms, analogues and protective approaches. *Crit Rev Toxicol.* 31, 55-138.
- 16 Bornehag, C.G., Reichenberg, A., Hallerback, M.U., Wikstrom, S., Koch, H.M., Jonsson, B.A., Swan,  
17 S.H., 2018. Prenatal exposure to acetaminophen and children's language development at 30  
18 months. *Eur Psychiatry.* 51, 98-103.
- 19 Bury, D., Modick-Biermann, H., Leibold, E., Brüning, T., Koch, H.M., 2019. Urinary metabolites of the  
20 UV filter octocrylene in humans as biomarkers of exposure. *Arch Toxicol.* 93, 1227-1238.
- 21 Chetwynd, A.J., Abdul-Sada, A., Hill, E.M., 2015. Solid-phase extraction and nanoflow liquid  
22 chromatography-nanoelectrospray ionization mass spectrometry for improved global urine  
23 metabolomics. *Anal Chem.* 87, 1158-65.
- 24 Cooper, A.J., Krasnikov, B.F., Niatsetskeya, Z.V., Pinto, J.T., Callery, P.S., Villar, M.T., Artigues, A.,  
25 Bruschi, S.A., 2011. Cysteine S-conjugate beta-lyases: important roles in the metabolism of  
26 naturally occurring sulfur and selenium-containing compounds, xenobiotics and anticancer  
27 agents. *Amino Acids.* 41, 7-27.
- 28 Cooper, A.J., Pinto, J.T., 2006. Cysteine S-conjugate beta-lyases. *Amino Acids.* 30, 1-15.
- 29 David, A., Abdul-Sada, A., Lange, A., Tyler, C.R., Hill, E.M., 2014. A new approach for plasma  
30 (xeno)metabolomics based on solid-phase extraction and nanoflow liquid chromatography-  
31 nanoelectrospray ionisation mass spectrometry. *J Chromatogr A.* 1365, 72-85.
- 32 David, A., Lange, A., Abdul-Sada, A., Tyler, C.R., Hill, E.M., 2017. Disruption of the Prostaglandin  
33 Metabolome and Characterization of the Pharmaceutical Exposome in Fish Exposed to  
34 Wastewater Treatment Works Effluent As Revealed by Nanoflow-Nanospray Mass  
35 Spectrometry-Based Metabolomics. *Environ Sci Technol.* 51, 616-624.
- 36 Djoumbou-Feunang, Y., Fiamoncini, J., Gil-de-la-Fuente, A., Greiner, R., Manach, C., Wishart, D.S.,  
37 2019a. BioTransformer: a comprehensive computational tool for small molecule metabolism  
38 prediction and metabolite identification. *J Cheminform.* 11, 2.
- 39 Djoumbou-Feunang, Y., Pon, A., Karu, N., Zheng, J., Li, C., Arndt, D., Gautam, M., Allen, F., Wishart,  
40 D.S., 2019b. CFM-ID 3.0: Significantly Improved ESI-MS/MS Prediction and Compound  
41 Identification. *Metabolites.* 9, 72.

1 Ferri, F.F., 2016. Ferri's clinical advisor 2017: 5 Books in 1. Elsevier Health Sciences : 1154–1155 ISBN  
2 9780323448383.

3 Gagnebin, Y., Tonoli, D., Lescuyer, P., Ponte, B., de Seigneux, S., Martin, P.-Y., Schappler, J., Boccard,  
4 J., Rudaz, S., 2017. Metabolomic analysis of urine samples by UHPLC-QTOF-MS: Impact of  
5 normalization strategies. *Analytica Chimica Acta*. 955, 27-35.

6 Gemborys, M.W., Mudge, G.H., 1981. Formation and disposition of the minor metabolites of  
7 acetaminophen in the hamster. *Drug Metab Dispos*. 9, 340-51.

8 Guijas, C., Montenegro-Burke, J.R., Domingo-Almenara, X., Palermo, A., Warth, B., Hermann, G.,  
9 Koellensperger, G., Huan, T., Uritboonthai, W., Aisporna, A.E., Wolan, D.W., Spilker, M.E.,  
10 Benton, H.P., Siuzdak, G., 2018. METLIN: A Technology Platform for Identifying Knowns and  
11 Unknowns. *Anal Chem*. 90, 3156-3164.

12 Hanna, P.E., Anders, M.W., 2019. The mercapturic acid pathway. *Crit Rev Toxicol*. 49, 819-929.

13 Hart, S.J., Healey, K., Smail, M.C., Calder, I.C., 1982. 3-thiomethylparacetamol sulphate and  
14 glucuronide: metabolites of paracetamol and N-hydroxyparacetamol. *Xenobiotica*. 12, 381-6.

15 Horai, H., Arita, M., Kanaya, S., Nihei, Y., Ikeda, T., Suwa, K., Ojima, Y., Tanaka, K., Tanaka, S.,  
16 Aoshima, K., Oda, Y., Kakazu, Y., Kusano, M., Tohge, T., Matsuda, F., Sawada, Y., Hirai, M.Y.,  
17 Nakanishi, H., Ikeda, K., Akimoto, N., Maoka, T., Takahashi, H., Ara, T., Sakurai, N., Suzuki, H.,  
18 Shibata, D., Neumann, S., Iida, T., Tanaka, K., Funatsu, K., Matsuura, F., Soga, T., Taguchi, R.,  
19 Saito, K., Nishioka, T., 2010. MassBank: a public repository for sharing mass spectral data for  
20 life sciences. *J Mass Spectrom*. 45, 703-14.

21 Hurwitz, J., Sands, S., Davis, E., Nielsen, J., Warholak, T., 2014. Patient knowledge and use of  
22 acetaminophen in over-the-counter medications. *J Am Pharm Assoc (2003)*. 54, 19-26.

23 Kanehisa, M., 2002. The KEGG database. *Novartis Found Symp*. 247, 91-101; discussion 101-3, 119-  
24 28, 244-52.

25 Kim, S., Chen, J., Cheng, T., Gindulyte, A., He, J., He, S., Li, Q., Shoemaker, B.A., Thiessen, P.A., Yu, B.,  
26 Zaslavsky, L., Zhang, J., Bolton, E.E., 2019. PubChem 2019 update: improved access to  
27 chemical data. *Nucleic Acids Res*. 47, D1102-d1109.

28 Konkel, L., 2018. Reproductive Headache? Investigating Acetaminophen as a Potential Endocrine  
29 Disruptor. *Environ Health Perspect*. 126, 032001.

30 Kortenkamp, A., 2020. Which chemicals should be grouped together for mixture risk assessments of  
31 male reproductive disorders? *Mol Cell Endocrinol*. 499, 110581.

32 Kortenkamp, A., Koch, H.M., 2020. Refined reference doses and new procedures for phthalate  
33 mixture risk assessment focused on male developmental toxicity. *International Journal of*  
34 *Hygiene and Environmental Health*. 224, 113428.

35 Kristensen, D.M., Desdoits-Lethimonier, C., Mackey, A.L., Dalgaard, M.D., De Masi, F., Munkbol, C.H.,  
36 Styrihave, B., Antignac, J.P., Le Bizec, B., Platel, C., Hay-Schmidt, A., Jensen, T.K., Lesne, L.,  
37 Mazaud-Guittot, S., Kristiansen, K., Brunak, S., Kjaer, M., Juul, A., Jegou, B., 2018. Ibuprofen  
38 alters human testicular physiology to produce a state of compensated hypogonadism. *Proc*  
39 *Natl Acad Sci U S A*. 115, E715-E724.

40 Kristensen, D.M., Lesne, L., Le Fol, V., Desdoits-Lethimonier, C., Dejuq-Rainsford, N., Leffers, H.,  
41 Jegou, B., 2012. Paracetamol (acetaminophen), aspirin (acetylsalicylic acid) and  
42 indomethacin are anti-androgenic in the rat foetal testis. *Int J Androl*. 35, 377-84.

43 Kristensen, D.M., Mazaud-Guittot, S., Gaudriault, P., Lesne, L., Serrano, T., Main, K.M., Jegou, B.,  
44 2016. Analgesic use - prevalence, biomonitoring and endocrine and reproductive effects. *Nat*  
45 *Rev Endocrinol*. 12, 381-93.

46 Larsen, G.L., 1985. Distribution of cysteine conjugate beta-lyase in gastrointestinal bacteria and in  
47 the environment. *Xenobiotica*. 15, 199-209.

48 Lessmann, F., Bury, D., Weiss, T., Hayen, H., Brüning, T., Koch, H.M., 2018. De-novo identification of  
49 specific exposure biomarkers of the alternative plasticizer di(2-ethylhexyl) terephthalate  
50 (DEHTP) after low oral dosage to male volunteers by HPLC-Q-Orbitrap-MS. *Biomarkers*. 23,  
51 196-206.

1 Mazaleuskaya, L.L., Sangkuhl, K., Thorn, C.F., FitzGerald, G.A., Altman, R.B., Klein, T.E., 2015.  
2 PharmGKB summary: pathways of acetaminophen metabolism at the therapeutic versus  
3 toxic doses. *Pharmacogenetics and genomics*. 25, 416-426.

4 Mikov, M., Caldwell, J., Dolphin, C.T., Smith, R.L., 1988. The role of intestinal microflora in the  
5 formation of the methylthio adduct metabolites of paracetamol. *Studies in neomycin-*  
6 *pretreated and germ-free mice*. *Biochem Pharmacol*. 37, 1445-9.

7 Modick, H., Schütze, A., Pälmeke, C., Weiss, T., Brüning, T., Koch, H.M., 2013. Rapid determination of  
8 N-acetyl-4-aminophenol (paracetamol) in urine by tandem mass spectrometry coupled with  
9 on-line clean-up by two dimensional turbulent flow/reversed phase liquid chromatography.  
10 *Journal of Chromatography B*. 925, 33-39.

11 Modick, H., Weiss, T., Dierkes, G., Bruning, T., Koch, H.M., 2014. Ubiquitous presence of paracetamol  
12 in human urine: sources and implications. *Reproduction*. 147, R105-17.

13 Modick, H., Weiss, T., Dierkes, G., Koslitz, S., Kafferlein, H.U., Bruning, T., Koch, H.M., 2016. Human  
14 metabolism and excretion kinetics of aniline after a single oral dose. *Arch Toxicol*. 90, 1325-  
15 33.

16 Nielsen, J.K., Modick, H., Morck, T.A., Jensen, J.F., Nielsen, F., Koch, H.M., Knudsen, L.E., 2015. N-  
17 acetyl-4-aminophenol (paracetamol) in urine samples of 6-11-year-old Danish school children  
18 and their mothers. *Int J Hyg Environ Health*. 218, 28-33.

19 Patterson, A.D., Carlson, B.A., Li, F., Bonzo, J.A., Yoo, M.H., Krausz, K.W., Conrad, M., Chen, C.,  
20 Gonzalez, F.J., Hatfield, D.L., 2013. Disruption of thioredoxin reductase 1 protects mice from  
21 acute acetaminophen-induced hepatotoxicity through enhanced NRF2 activity. *Chem Res*  
22 *Toxicol*. 26, 1088-96.

23 Pence, H.E., Williams, A., 2010. ChemSpider: An Online Chemical Information Resource. *Journal of*  
24 *Chemical Education*. 87, 1123-1124.

25 Roberts, M.S., Magnusson, B.M., Burczynski, F.J., Weiss, M., 2002. Enterohepatic Circulation. *Clinical*  
26 *Pharmacokinetics*. 41, 751-790.

27 Rohart, F., Gautier, B., Singh, A., KA, L.C., 2017. mixOmics: An R package for 'omics feature selection  
28 and multiple data integration. *PLoS Comput Biol*. 13, e1005752.

29 Ruttkies, C., Schymanski, E.L., Wolf, S., Hollender, J., Neumann, S., 2016. MetFrag relaunched:  
30 incorporating strategies beyond in silico fragmentation. *Journal of cheminformatics*. 8, 3-3.

31 Schulz, M., Iwersen-Bergmann, S., Andresen, H., Schmoldt, A., 2012. Therapeutic and toxic blood  
32 concentrations of nearly 1,000 drugs and other xenobiotics. *Crit Care*. 16, R136.

33 Schymanski, E.L., Jeon, J., Gulde, R., Fenner, K., Ruff, M., Singer, H.P., Hollender, J., 2014. Identifying  
34 small molecules via high resolution mass spectrometry: communicating confidence. *Environ*  
35 *Sci Technol*. 48, 2097-8.

36 Smith, C.A., Want, E.J., O'Maille, G., Abagyan, R., Siuzdak, G., 2006. XCMS: processing mass  
37 spectrometry data for metabolite profiling using nonlinear peak alignment, matching, and  
38 identification. *Anal Chem*. 78, 779-87.

39 Sumner, L.W., Amberg, A., Barrett, D., Beale, M.H., Beger, R., Daykin, C.A., Fan, T.W., Fiehn, O.,  
40 Goodacre, R., Griffin, J.L., Hankemeier, T., Hardy, N., Harnly, J., Higashi, R., Kopka, J., Lane,  
41 A.N., Lindon, J.C., Marriott, P., Nicholls, A.W., Reily, M.D., Thaden, J.J., Viant, M.R., 2007.  
42 Proposed minimum reporting standards for chemical analysis Chemical Analysis Working  
43 Group (CAWG) Metabolomics Standards Initiative (MSI). *Metabolomics*. 3, 211-221.

44 Want, E.J., Wilson, I.D., Gika, H., Theodoridis, G., Plumb, R.S., Shockcor, J., Holmes, E., Nicholson, J.K.,  
45 2010. Global metabolic profiling procedures for urine using UPLC-MS. *Nature Protocols*. 5,  
46 1005.

47 Wishart, D., Arndt, D., Pon, A., Sajed, T., Guo, A.C., Djoumbou, Y., Knox, C., Wilson, M., Liang, Y.,  
48 Grant, J., Liu, Y., Goldansaz, S.A., Rappaport, S.M., 2015. T3DB: the toxic exposome  
49 database. *Nucleic Acids Res*. 43, D928-34.

50 Wishart, D.S., Feunang, Y.D., Guo, A.C., Lo, E.J., Marcu, A., Grant, J.R., Sajed, T., Johnson, D., Li, C.,  
51 Sayeeda, Z., Assempour, N., Iynkkaran, I., Liu, Y., Maciejewski, A., Gale, N., Wilson, A., Chin,

1 L., Cummings, R., Le, D., Pon, A., Knox, C., Wilson, M., 2018a. DrugBank 5.0: a major update  
2 to the DrugBank database for 2018. *Nucleic Acids Res.* 46, D1074-d1082.  
3 Wishart, D.S., Feunang, Y.D., Marcu, A., Guo, A.C., Liang, K., Vázquez-Fresno, R., Sajed, T., Johnson,  
4 D., Li, C., Karu, N., Sayeeda, Z., Lo, E., Assempour, N., Berjanskii, M., Singhal, S., Arndt, D.,  
5 Liang, Y., Badran, H., Grant, J., Serra-Cayuela, A., Liu, Y., Mandal, R., Neveu, V., Pon, A., Knox,  
6 C., Wilson, M., Manach, C., Scalbert, A., 2018b. HMDB 4.0: the human metabolome database  
7 for 2018. *Nucleic Acids Res.* 46, D608-d617.

8

9

10